Static versus energy-dependent nucleus–nucleus potential for description of sub-barrier fusion dynamics of $^{16}_{8}$O+$^{112,116,120}_{50}$Sn reactions*

Manjeet Singh Gautam[1)]

School of Physics and Material Science, Thapar University, Patiala (Punjab)-147004, India

Abstract: The static and energy-dependent nucleus–nucleus potentials are simultaneously used along with the Wong formula for exploration of fusion dynamics of $^{16}_{8}$O+$^{112,116,120}_{50}$Sn reactions. The role of internal structure degrees of freedom of colliding pairs, such as inelastic surface vibrations, are examined within the context of coupled channel calculations performed using the code CCFULL. Theoretical calculations based on the static Woods–Saxon potential along with the one-dimensional Wong formula fail to address the fusion data of $^{16}_{8}$O+$^{112,116,120}_{50}$Sn reactions. Such discrepancies can be removed if one uses couplings to internal structure degrees of freedom of colliding nuclei. However, the energy-dependent Woods–Saxon potential model (EDWSP model) accurately describes the sub-barrier fusion enhancement of $^{16}_{8}$O+$^{112,116,120}_{50}$Sn reactions. Therefore, in sub-barrier fusion dynamics, energy dependence in the nucleus–nucleus potential governs barrier modification effects in a closely similar way to that of the coupled channel approach.

Key words: heavy-ion sub-barrier fusion reactions, depth and diffuseness, Woods–Saxon potential, diffuseness anomaly

PACS: 25.60.Pj, 21.60.Ev, 24.10.Eq **DOI:** 10.1088/1674-1137/39/11/114102

1 Introduction

The understanding of the rich interplay of nuclear structure and nuclear interactions in the dynamics of fusion reactions has been a subject of theoretical and experimental interest in the past few decades. Heavy ion fusion cross-sections in the close vicinity of the Coulomb barrier are strongly influenced by the coupling of relative motion with the nuclear structure degrees of freedom such as inelastic surface excitations of the projectile (target) or permanent deformations of the projectile (target) and/or nucleon (multi-nucleon) transfer channels. These couplings produce substantially large fusion enhancement at sub-barrier energies and the measured fusion cross-section data are found to be larger by several orders of magnitude than the predictions of the one-dimensional barrier penetration model [1–4]. The inelastic surface excitations of colliding nuclei, static deformations and the nucleon transfer degrees are found to be the dominating mode of couplings which can be partially or fully manifested for sub-barrier fusion enhancement. The effect of coupling between the elastic channel and intrinsic degrees of freedom is to replace the single Coulomb barrier with a barrier distribution and thus results in an anomalously large sub-barrier fusion enhancement. The static and dynamical physical effects that arise due to permanent shape deformation and inelastic surface excitations are adequately addressed by the various theoretical models [1–7]. However, the situation is quite different in neutron-rich nuclei, wherein due to the larger number of neutrons and larger nuclear size, the magnitude of fusion cross-section is quite large compared to that of stable isotopes. It is very difficult to establish the precise effects of nucleon transfer channels on fusion dynamics because such processes occur at much larger inter-nucleon separation and involve a complex rearrangement of nucleons between fusing nuclei [8–15].

Theoretically, in reaction dynamics, the impact of various static and dynamical physical effects is imparted through the nucleus–nucleus potential. The accurate picture of this potential, which plays a central role in the nuclear reaction dynamics, greatly simplifies the problem of basic understanding of nuclear interaction between collision partners. The sum of repulsive Coulomb interaction and short ranged attractive nuclear interaction forms a fusion barrier which must be overcome for the fusion

Received 27 March 2015

∗ Supported by Dr. D. S. Kothari Post-Doctoral Fellowship Scheme sponsored by University Grants Commission (UGC), New Delhi, India

1) E-mail: gautammanjeet@gmail.com

©2015 Chinese Physical Society and the Institute of High Energy Physics of the Chinese Academy of Sciences and the Institute of Modern Physics of the Chinese Academy of Sciences and IOP Publishing Ltd

process to occur [16, 17]. The success of any theoretical formulation is very sensitive to the choice of the optimum form of nucleus–nucleus potential. In realistic calculations such as coupled channel calculations, the nuclear potential not only affects the width of the fusion barrier but also regulates the nuclear coupling strengths. Therefore, the choice of nuclear potential directly or indirectly influences the theoretical results of fusion excitation function and related phenomenon. Because of the existence of large ambiguities in the optimum choice of nucleus–nucleus potential, various aspects of sub-barrier fusion dynamics are still unexplored. To explain the different nuclear interactions, large numbers of parameterizations of nuclear potential are available in the literature, and are regularly used in connection with nuclear reaction studies [18–24]. Generally, the static Woods–Saxon potential, which is controlled by three parameters—depth, range and diffuseness—is used to describe the dynamics of the fusion process. The diffuseness parameter of this potential is related to the slope of the nuclear potential in the tail region of the Coulomb barrier and hence affects the barrier width as well as channel coupling strengths. In the literature, there is a large amount of experimental evidence wherein significantly larger values of the diffuseness parameter, ranging from $a=0.75$ fm to $a=1.5$ fm, are used for a complete description of the sub-barrier fusion data. Surprisingly, such values are much larger than the value (a=0.65 fm) deduced from the systematics of elastic scattering data [25–29]. Furthermore, at deep sub-barrier energies, the slope of the fusion excitation function falls more steeply than predicted by the nuclear potential, with a diffuseness of a=0.65 fm. This steep fall of fusion cross-section data can only be addressed if one uses abnormally large diffuseness ranging from a=0.75 fm to a=1.5 fm. These observations seem to be a general trend of fusion dynamics in medium mass heavy ion systems [7]. This diffuseness anomaly, which might be an artifact of different kinds of static and dynamical physical effects, reflects the systematic failure of the static Woods–Saxon potential in simultaneous exploration of the elastic scattering and the fusion data [1–7, 25–29]. To understand the cause of the diffuseness anomaly and the puzzling behavior of sub-barrier fusion dynamics, our previous work has undertaken several attempts to study the fusion process within the framework of the energy-dependent Woods–Saxon potential model (EDWSP model) [30–41]. In heavy ion reactions, the closely similar physical effects that arise due to the internal structure of colliding pairs can be induced by incorporating the energy-dependence in the real part of the nucleus–nucleus potential so that it becomes more attractive at sub-barrier energies. This energy-dependent nucleus–nucleus potential will effectively decrease the interaction barrier between fusing nuclei (see Fig. 2) and hence predicts a substantially larger sub-barrier fusion cross-section in comparison to the energy-independent one-dimensional barrier penetration model [30–41].

Generally, the order of sub-barrier fusion enhancement increases with increase of neutron richness because of the possibility of neutron (multi-neutron) transfer channels. However, in the fusion of ${}^{16}_{8}\mathrm{O}+{}^{112,116,120}_{50}\mathrm{Sn}$ systems, besides the large N/Z ratio, neither of the projectile-target combinations facilitates the neutron transfer channel with positive ground state Q-values [42–44]. Although all the Sn-isotopes are similar in nuclear shell structure, strong isotopic fusion enhancement is expected for the neutron-rich target isotope (${}^{116,120}_{50}\mathrm{Sn}$). However, the fusion dynamics of ${}^{16}_{8}\mathrm{O}+{}^{112,116,120}_{50}\mathrm{Sn}$ systems have a dominance of multi-phonon vibrational states and hence show weak rather than strong target isotopic dependence of sub-barrier fusion enhancement. Theoretical calculations are performed using the energy-independent Woods–Saxon potential as well as the energy-dependent Woods–Saxon potential model in conjunction with the one-dimensional Wong formula [45]. The role of inelastic surface vibrational states of target isotopes are included within the context of coupled channel calculations performed using the code CCFULL [46]. Furthermore, the failure of the static Woods–Saxon potential along with the Wong formula to explain the fusion of ${}^{16}_{8}\mathrm{O}+{}^{112,116,120}_{50}\mathrm{Sn}$ systems reflects its limitations for exploration of sub-barrier fusion data. However, the EDWSP model adequately describes the fusion enhancement of these systems, with the energy dependence in the Woods–Saxon potential introducing barrier modification effects (barrier position, barrier height, barrier curvature) in a somewhat similar way to that of coupled channel formulation and hence simulating various channel coupling effects that arise due to the internal structure degrees of colliding nuclei. A brief description of the method of calculation is given in Section 2. The results are discussed in detail in Section 3 while the conclusions drawn are discussed in Section 4.

2 Theoretical formalism

2.1 One-dimensional Wong formula

The partial wave fusion cross-section is given as

$$\sigma_{\mathrm{F}}=\frac{\pi}{k^2}\sum_{\ell=0}^{\infty}(2\ell+1)T_{\ell}^{\mathrm{F}}, \tag{1}$$

Hill and Wheeler proposed an expression for tunneling probability (T_{ℓ}^{F}) which is based upon the parabolic approximation, wherein the effective interaction between

the collision partners has been replaced by an inverted parabola [1–7, 30–41, 47].

$$T_\ell^{\rm HW}=\frac{1}{1+\exp\left[\frac{2\pi}{\hbar\omega_\ell}(V_\ell-E)\right]}. \quad (2)$$

Using Wong's approximations in the above expression and assuming that an infinite number of partial waves contribute to the fusion process, one can obtain the following final expression for the Wong formula for evaluating the fusion excitation function [1–7, 30–41, 45].

$$\sigma_{\rm F}=\frac{\hbar\omega R_{\rm B}^2}{2E}\ln\left[1+\exp\left(\frac{2\pi}{\hbar\omega}(E-V_{\rm B})\right)\right]. \quad (3)$$

2.2 Energy-dependent Woods–Saxon Potential model (EDWSP model)

The nucleus–nucleus potential, which defines the fundamental characteristic of heavy ion fusion reactions, is one of the most important inputs for theoretical models. In the present study, both the static Woods–Saxon potential and the energy-dependent Woods–Saxon potential in conjunction with the one-dimensional Wong formula are used for theoretical calculations [30–41]. In addition, the static Woods–Saxon potential has been used in the coupled channel calculations. The form of the static Woods–Saxon potential is defined as

$$V_{\rm N}(r)=\frac{-V_0}{\left[1+\exp\left(\frac{r-R_0}{a}\right)\right]}, \quad (4)$$

with, $R_0=r_0(A_{\rm P}^{\frac{1}{3}}+A_{\rm T}^{\frac{1}{3}})$. The quantity '$V_0$' is depth and '$a$' is the diffuseness parameter of the nuclear potential. In the EDWSP model, the depth of the real part of the Woods–Saxon potential is defined as [30–41].

$$V_0 = \left[A_{\rm P}^{\frac{2}{3}}+A_{\rm T}^{\frac{2}{3}}-(A_{\rm P}+A_{\rm T})^{\frac{2}{3}}\right] \times\left[2.38+6.8(1+I_{\rm P}+I_{\rm T})\frac{A_{\rm P}^{\frac{1}{3}}A_{\rm T}^{\frac{1}{3}}}{\left(A_{\rm P}^{\frac{1}{3}}+A_{\rm T}^{\frac{1}{3}}\right)}\right] \text{ MeV}, \quad (5)$$

where $I_{\rm P}=\left(\frac{N_{\rm P}-Z_{\rm P}}{A_{\rm P}}\right)$ and $I_{\rm T}=\left(\frac{N_{\rm T}-Z_{\rm T}}{A_{\rm T}}\right)$ are the isospin asymmetry of collision partners. This parameterization of depth has been obtained by reproducing the fusion excitation function data of a large number of heavy ion fusion reactions ranging from $Z_{\rm P}Z_{\rm T}=84$ to $Z_{\rm P}Z_{\rm T}=1640$ [30–41]. In fusion dynamics, the various kinds of static and dynamical physical effects such as variations of N/Z ratio, variations of surface energy and surface diffuseness of colliding pairs, variations of nucleon densities in the neck region and dissipation of kinetic energy of relative motion to internal structure degrees of freedom of fusing nuclei occur in the surface region of the nuclear potential or in the tail region of the Coulomb barrier. In addition, if a common projectile is bombarded on a series of target isotopes or vice versa, the isotopic effects are directly evident and must be included in the calculations. All these physical effects induce a modification in the parameters of the static Woods–Saxon potential and hence bring the requirement of a larger diffuseness parameter ranging from a=0.75 fm to a=1.5 fm to account for sub-barrier fusion data [1–7, 25–29]. In this regard, the energy-dependent Woods–Saxon potential was proposed in our previous work [30–41], as it takes care of various kinds of static and dynamical physical effects via its diffuseness parameter, which is taken as energy-dependent and hence defined as

$$a(E)=0.85\left[1+\frac{r_0}{13.75\left(A_{\rm P}^{-\frac{1}{3}}+A_{\rm T}^{-\frac{1}{3}}\right)\left(1+\exp\left(\frac{\frac{E}{V_{\rm B0}}-0.96}{0.03}\right)\right)}\right] \text{fm}. \quad (6)$$

It is worth noting here that the value of the diffuseness parameter strongly depends upon the nature of the interacting nuclei and the bombarding energy of the colliding nuclei. The range parameter r_0 is treated as a free parameter in order to vary the diffuseness parameter. In the present work, it can easily be noticed that the theoretical calculations based upon the static Woods–Saxon potential must incorporate the couplings to internal nuclear structure degrees of freedom, such as inelastic surface excitations of colliding pairs, rotational states of deformed nuclei and multi-nucleon transfer channels or other static and dynamical effects to reproduce the sub-barrier fusion data. However, the energy dependence in the nucleus–nucleus potential governs similar kinds of channel coupling effects that arise due to the coupling of relative motion of reactants to internal structure degrees of freedom, and thus reasonably accounts for the sub-barrier fusion excitation function data. The underlying reason for equivalency of these two different physical mechanisms (EDWSP model and coupled channel

approach) is that both produce similar kinds of barrier modification effects (barrier height, barrier position, barrier curvature) in the heavy ion fusion reactions.

2.3 Coupled channel model

This section briefly reviews the details of the coupled channel approach which is used to analyze the fusion dynamics of various heavy ion fusion reactions. Theoretically, the standard way to address the impact of internal structure degrees of freedom of fusing nuclei is to solve the coupled channel equations. In coupled channel calculations, it is very difficult to entertain the effects of all intrinsic channels simultaneously but one can reasonably include the relevant channels [30–41, 46, 48–52]. Therefore, the set of coupled channel equations can be written as

$$\left[\frac{-\hbar^2}{2\mu}\frac{\mathrm{d}^2}{\mathrm{d}r^2}+\frac{J(J+1)\hbar^2}{2\mu r^2}+V_{\mathrm{N}}(r)+\frac{Z_{\mathrm{P}}Z_{\mathrm{T}}e^2}{r}+\varepsilon_n-E_{\mathrm{cm}}\right]\times\psi_{\mathrm{n}}(r)+\sum_m V_{nm}(r)\psi_m(r)=0, \tag{7}$$

where, $\vec{r}$ is the radial coordinate representing the relative motion between fusing nuclei; μ is the reduced mass of the colliding system; E_{cm} and ε_n represents the bombarding energy in the centre-of-mass frame and the excitation energy of the n^{th} channel respectively; and V_{nm} are the matrix elements of the coupling Hamiltonian, which in the collective model consists of Coulomb and nuclear components. The coupled channel calculations are done by using the code CCFULL [46] wherein the coupled channel equations are solved numerically by adopting two basic approximations. The first approximation is the no-Coriolis or rotating frame approximation which has been used to reduce the number of coupled channel equations [30–41, 46, 48–52]. If there is no transfer of angular momentum from the relative motion of colliding nuclei to their intrinsic motion, the total orbital angular momentum quantum number L can be replaced by the total angular momentum quantum number J and hence leads to a great reduction in the number of coupled channel equations. The second approximation is ingoing wave boundary conditions (IWBC), which is highly applicable to heavy ion reactions. According to IWBC, there are only incoming waves at $r=r_{\mathrm{min}}$, which is taken as the minimum position of the Coulomb pocket inside the barrier, and there are only outgoing waves at infinity for all channels except the entrance channel ($n=0$). By entertaining the effects of all relevant internal degrees of freedom, the fusion cross-section becomes

$$\sigma_{\mathrm{F}}(E)=\sum_J\sigma_J(E)=\frac{\pi}{k_0^2}\sum_J(2J+1)P_J(E), \tag{8}$$

where $P_J(E)$ is the total transmission coefficient corresponding to the angular momentum J.

3 Results and discussion

The values of the deformation parameters and their corresponding excitation energies for low lying 2^+ and 3^- vibrational states of all these nuclei are listed in Table 1. The barrier height, barrier position and barrier curvature of the fusing nuclei used in the EDWSP model calculations are listed in Table 2. The values of range, depth and diffuseness of EDWSP model for various combinations of projectile and target are listed in Table 3.

Table 1. The deformation parameter (β_λ) and the energy (E_λ) of the quadrupole and octupole vibrational states of fusing nuclei.

nucleus	β_2	E_2/MeV	β_3	E_3/MeV	reference
$^{16}_{8}$O	0.362	6.917	0.370	6.129	[42]
$^{112}_{50}$Sn	0.158	1.256	0.185	2.354	[42]
$^{116}_{50}$Sn	0.143	1.293	0.213	2.266	[42]
$^{120}_{50}$Sn	0.137	1.170	0.176	2.400	[42]

Table 2. The values of V_{B0}, R_{B} and $\hbar\omega$ used in the EDWSP model calculations for various heavy ion fusion reactions.

system	V_{B0}/MeV	R_{B}/fm	$\hbar\omega$/MeV	reference
$^{16}_{8}$O+$^{112}_{50}$Sn	51.35	10.27	3.81	[42]
$^{16}_{8}$O+$^{116}_{50}$Sn	50.94	10.36	3.78	[42]
$^{16}_{8}$O+$^{120}_{50}$Sn	50.41	10.73	4.37	[44]

Table 3. Range, depth and diffuseness of Woods–Saxon potential used in the EDWSP model calculations for various heavy ion fusion reactions [30–41].

system	r_0/fm	V_0/MeV	$\frac{a^{\mathrm{present}}}{\text{energy range}}\Big/\left(\frac{\text{fm}}{\text{MeV}}\right)$
$^{16}_{8}$O+$^{112}_{50}$Sn	1.122	62.11	$\frac{0.96\text{ to }0.85}{40\text{ to }65}$
$^{16}_{8}$O+$^{116}_{50}$Sn	1.125	64.14	$\frac{0.96\text{ to }0.85}{40\text{ to }65}$
$^{16}_{8}$O+$^{120}_{50}$Sn	1.128	66.07	$\frac{0.96\text{ to }0.85}{40\text{ to }65}$

In the fusion dynamics of $^{16}_{8}$O+$^{112,116,120}_{50}$Sn systems, the couplings to two phonon inelastic surface excitations of target isotopes are sufficient to account for the sub-barrier fusion enhancement over the prediction of one dimensional barrier penetration model. The projectile is a doubly magic nucleus and its low lying surface vibrational states like 2^+ and 3^- vibrational states lie at high excitation energies and hence do not play any role in the fusion mechanism of $^{16}_{8}$O+$^{112,116,120}_{50}$Sn systems. In addition, the common projectile contributes equally to three reactions, so the distinguishing features of energy dependence of low energy fusion data can be attributed to the slightly different collective properties of the target

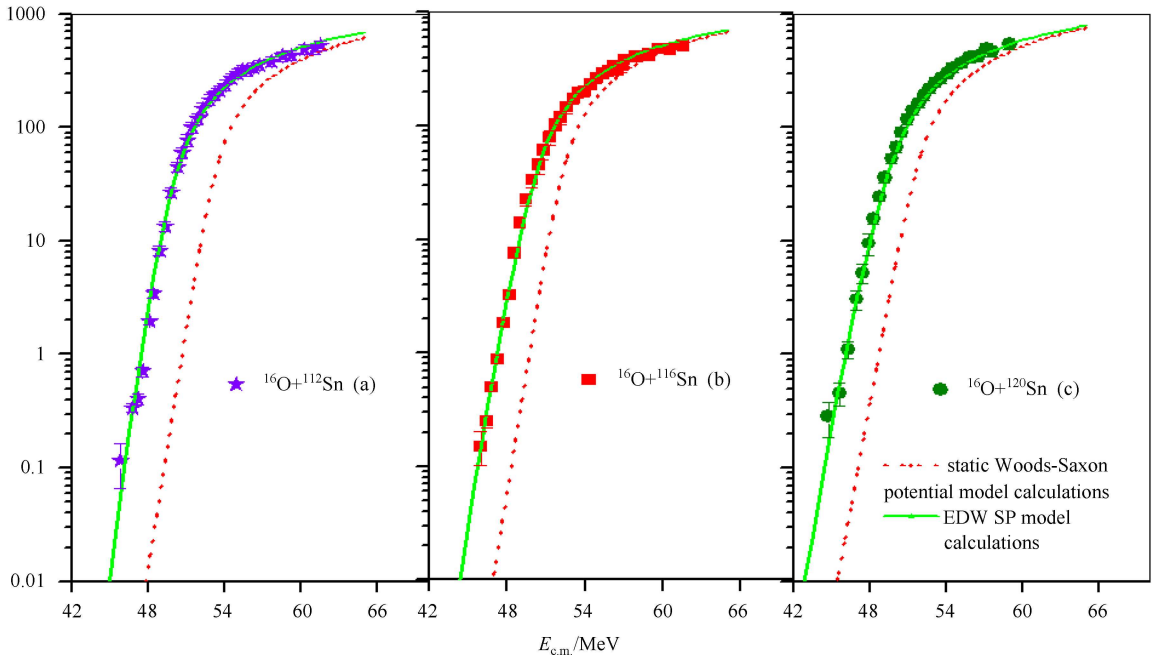

Fig. 1. (color online) The fusion excitation functions of $^{16}_{8}$O+$^{112,116,120}_{50}$Sn systems obtained using the static Woods–Saxon potential model and the energy-dependent Woods–Saxon potential model (EDWSP model) [30–41]. The results are compared with available experimental data (Symbols) taken from Refs. [42–44].

nuclei. The details of coupled channel calculations will be discussed in Fig. 3. The fusion dynamics of $^{16}_{8}$O+ $^{112,116,120}_{50}$Sn systems are analyzed using the static Woods–Saxon potential and the energy-dependent Woods–Saxon potential model (EDWSP model) in conjunction with the one-dimensional Wong formula. In the fusion of $^{16}_{8}$O+$^{112,116,120}_{50}$Sn systems, the theoretical calculations based on the static Woods–Saxon potential are significantly smaller than the results of experimental data. This indicates that the static Woods–Saxon potential is not suitable to describe sub-barrier fusion dynamics. However, when the scenarios of fusion dynamics of these fusing systems are considered within the context of the EDWSP model, it adequately explains the sub-barrier fusion excitation function data, as is evident from Fig. 1.

In the EDWSP model, the energy-dependent diffuseness parameter produces barrier modification effects and hence leads to a distribution of barrier of varying height, as shown in Fig. 2. Some of the barriers have heights lower than that of the Coulomb barrier, which leads to a transfer of incoming flux from elastic channel to fusion channel. This ultimately predicts larger sub-barrier fusion excitation functions over the expectation of the energy-independent one-dimensional Wong formula. It is very interesting to note that the variation of diffuseness parameter is effectively equivalent to an increase of capture radii of colliding nuclei, which in turn suggests that the fusion process starts at much larger inter-nuclear separation between the collision partners [31]. In the EDWSP model calculations, a=0.96 fm is the largest diffuseness that produces the lowest fusion barrier which can be ascribed to the larger fusion enhancement at sub-barrier energies. For instance, in the fusion of the $^{16}_{8}$O+$^{120}_{50}$Sn system, the lowest fusion barrier produced at the largest diffuseness parameter (a=0.96 fm) is 48.24 MeV, as shown in Fig. 2(b). This fusion barrier is much smaller than that of the Coulomb barrier (50.41 MeV) which is obtained using the static Woods–Saxon potential, and because of the lower fusion barrier, enhancement of fusion excitation function at below-barrier energies is directly evident. The difference between the lowest fusion barrier produced in the EDWSP model calculations and the Coulomb barrier is 2.17 MeV. As the bombarding energy increases, the value of the diffuseness parameter decreases from a=0.96 fm to a=0.85 fm, resulting in an increase of the height of the corresponding fusion barrier from 48.24 MeV to 49.69 MeV. In above-barrier energy regions, where the fusion cross-section is almost independent of different channel coupling effects (internal structure of colliding nuclei), the diffuseness parameter gets saturated to its minimum value (a=0.85 fm). At this diffuseness, the corresponding fusion barrier is highest (49.69 MeV), as evident from Fig. 2. This fusion barrier is still smaller than that of the Coulomb barrier. Similar results are found for $^{16}_{8}$O+$^{112,116}_{50}$Sn systems. In the coupled channel calculations of $^{16}_{8}$O+$^{112,116,120}_{50}$Sn systems, which will be discussed in Fig. 3, the inclusions of rea-

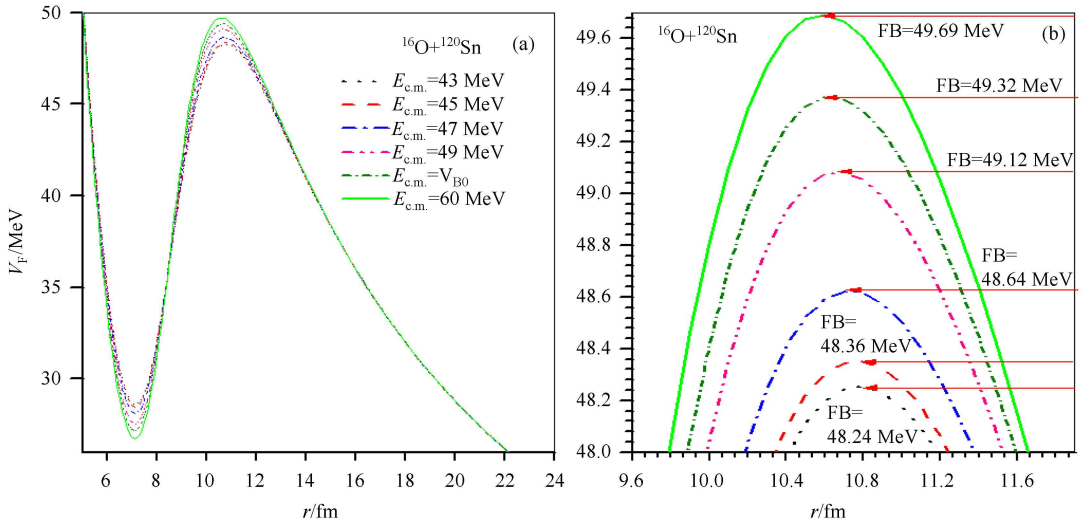

Fig. 2. (color online) The fusion barrier (FB) for $^{16}_{8}$O+$^{120}_{50}$Sn system obtained using the EDWSP model [30–41]. Similar results are found in the fusion of $^{16}_{8}$O+$^{112,116}_{50}$Sn systems.

sonably inelastic surface excitations of target isotopes reproduce the sub-barrier fusion mechanism, which clearly indicates that channel coupling effects lead to the reduction of the Coulomb barrier and thus are responsible for the maximum flux lost from elastic channel to fusion channel. It is worth noting here that as the diffuseness of the static Woods–Saxon potential increases, the potential pocket becomes shallower and at significantly larger diffuseness parameter ($a \geqslant$1.0 fm depending on the nature of the colliding system), the potential pocket almost disappears and hence limits the occurrence of the fusion process. However, in the EDWSP model, although the potential becomes shallower with increase of diffuseness, a well-defined potential pocket still exists even at large values of diffuseness parameter (a=0.96 fm), as shown in Fig. 2(a). The realistic coupled channel calculations (CCFULL calculations) make use of ingoing wave boundary conditions which are very sensitive to the existence of the potential pocket and require a deeper potential for addressing heavy ion fusion reactions. On the other hand, in the EDWSP model calculations, due to the energy dependence of diffuseness, various kinds of static and dynamical physical effects are included and the existence of the potential pocket is regulated even at large diffuseness, and hence similar barrier modification effects are introduced as reflected from the coupled channel analysis.

In the fusion of $^{16}_{8}$O+$^{112,116}_{50}$Sn systems, no-coupling calculations wherein both collision partners are taken as inert are significantly smaller than the experimental fusion data. The projectile has low lying surface vibrational states, but due to high excitation energies the fusion dynamics of these systems remain almost insensitive to the inclusion of vibrational state of the projectile. Therefore, in the present analysis, the vibrational states of projectiles are not included in the coupled channel calculations, while the inelastic surface excitation of target nuclei are taken into account. The inclusion of one-phonon 2^+ vibrational state alone or 3^- vibrational states in target alone enhances the sub-barrier fusion cross-section over the no-coupling calculations but is unable to account the experimental data. The coupling to one-phonon 2^+ and 3^- vibrational states in the target, along with their mutual coupling, produces the larger fusion cross-section at below-barrier energies, but besides this the theoretical results fail to bring observed fusion enhancement. This suggests that higher multi-phonon vibrational states of target nuclei must be incorporated for complete description of experimental fusion data. The additions of two-phonon 2^+ and 3^- vibrational states in the target along with their mutual coupling reasonably accounts for the sub-barrier fusion enhancement, as shown in Fig. 3. The inclusion of mutual coupling vibrational states such as 2^+, 3^-, $(2^+)^2$, $(3^-)^2$ and $(2^+\otimes 3^-)$vibrational states further improves the theoretical results. The further additions of higher order vibrational states, like three-phonon and four-phonon states, do not bring any additional enhancement at below-barrier energies and hence couplings to up to two-phonon vibrational states of target nuclei in the fusion of $^{16}_{8}$O+$^{112,116}_{50}$Sn systems adequately address the fusion enhancement at sub-barrier energies.

In the fusion of $^{16}_{8}$O+$^{120}_{50}$Sn system, the same coupling scheme as for $^{16}_{8}$O+$^{112,116}_{50}$Sn reactions reasonably reproduces the energy dependence of fusion cross-section data where the couplings to inelastic surface vibrational states such as one-phonon, and two-phonon vibrational states enhances the magnitude of fusion cross-section data over

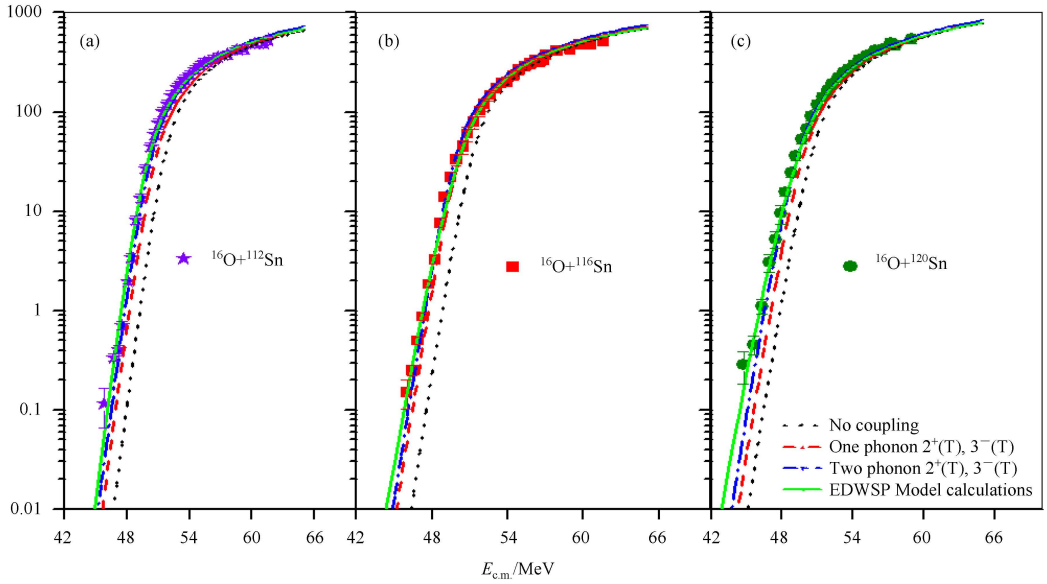

Fig. 3. (color online) The fusion excitation functions of $^{16}_{8}$O+$^{112,116,120}_{50}$Sn systems obtained using the EDWSP model [30–41] and the coupled channel code CCFULL [46]. The results are compared with available experimental data (Symbols) taken from Ref. [42–44].

the no-coupling calculations. The inclusions of one phonon 2^+ and 3^-vibrational states along with their mutual coupling in the target is unable to reproduce the sub-barrier fusion data, while the double phonon vibrational states along with their mutual coupling like 2^+, 3^-, $(2^+)^2$, $(3^-)^2$ and $(2^+\otimes 3^-)$ vibrational states accurately address the sub-barrier fusion data. The sub-barrier fusion dynamics is almost insensitive to further addition of more intrinsic excitations of the target nucleus. The fusion enhancement of the $^{16}_{8}$O+$^{120}_{50}$Sn system is found to be larger than that of $^{16}_{8}$O+$^{112,116}_{50}$Sn systems. This additional fusion enhancement at sub-barrier energies can be understood in terms of strong collective properties of the $^{120}_{50}$Sn nucleus. As far as the nuclear structure of Sn-isotopes is concerned, all the Sn-isotopes are similar in nature but due to large neutron richness, strong isotopic dependence of fusion enhancement is expected for $^{16}_{8}$O+$^{116,120}_{50}$Sn systems. The deformation parameter and their corresponding excitation energies are similar but the larger sub-barrier fusion enhancement of $^{16}_{8}$O+$^{120}_{50}$Sn system with respect to $^{16}_{8}$O+$^{112,116}_{50}$Sn systems can be understood in terms of low excitation energy of quadrupole vibrations of $^{120}_{50}$Sn-nucleus in comparison with $^{112,116}_{50}$Sn nuclei (see Table 1). Therefore, the sub-barrier fusion enhancement of these systems in comparison to the predications of the one-dimensional barrier penetration model can only be correlated with dominance of inelastic surface excitations of target isotopes.

The fusion cross-section data of $^{16}_{8}$O+$^{112,116,120}_{50}$Sn show weak isotopic dependence because of unavailability of the neutron transfer channel with positive ground state Q-values. Besides the increase of N/Z ratio of target isotopes with increase of isotopic mass, neither of the fusing systems offers a nucleon transfer channel with positive ground state Q-value. For instance, the N/Z ratio of the Sn target nuclei are 1.24, 1.32 and 1.4 for $^{112}_{50}$Sn, $^{116}_{50}$Sn and $^{120}_{50}$Sn respectively. In addition, the entrance channel mass asymmetry effects of $^{16}_{8}$O+$^{112,116,120}_{50}$Sn systems also increase with neutron richness. The size of the neck formed between the colliding nuclei leading to the formation of the same compound nucleus strongly depends on the entrance channel mass asymmetry effect. In Ref. [53], the authors clearly showed that the fusion inhibition factor decreases with increase of entrance channel mass asymmetry, and larger entrance channel mass asymmetry favors the fusion process. As discussed in Refs. [12, 31], the fusion of the $^{46}_{22}$Ti+$^{64}_{28}$Ni system and $^{50}_{22}$Ti+$^{60}_{28}$Ni system leads to the formation of the same compound nucleus $^{110}_{50}$Sn and the larger sub-barrier fusion enhancement of the $^{46}_{22}$Ti+$^{64}_{28}$Ni system in comparison to the $^{50}_{22}$Ti+$^{60}_{28}$Ni system can be correlated with the larger entrance channel mass asymmetry of the former fusing system. Therefore, the magnitude of sub-barrier fusion enhancement should increase with the increase of entrance channel mass asymmetry (η). For instance, the $^{16}_{8}$O+$^{112}_{50}$Sn system has $\eta=\left|\frac{A_{\rm P}-A_{\rm T}}{A_{\rm P}+A_{\rm T}}\right|=0.750$, the $^{16}_{8}$O+$^{116}_{50}$Sn system has $\eta=\left|\frac{A_{\rm P}-A_{\rm T}}{A_{\rm P}+A_{\rm T}}\right|=0.757$ and the $^{16}_{8}$O+$^{120}_{50}$Sn system has $\eta=\left|\frac{A_{\rm P}-A_{\rm T}}{A_{\rm P}+A_{\rm T}}\right|=0.764$. It is expected that a larger mass-asymmetric fusing system produces a larger

sub-barrier fusion enhancement with respect to a less mass-asymmetric fusing system. Therefore, the larger fusion excitation function of the $^{16}_{8}$O+$^{120}_{50}$Sn system in comparison to the $^{16}_{8}$O+$^{112,116}_{50}$Sn systems can also be correlated to the larger entrance channel mass asymmetry effects and the larger N/Z ratio of the target isotope, as depicted in Fig. 4.

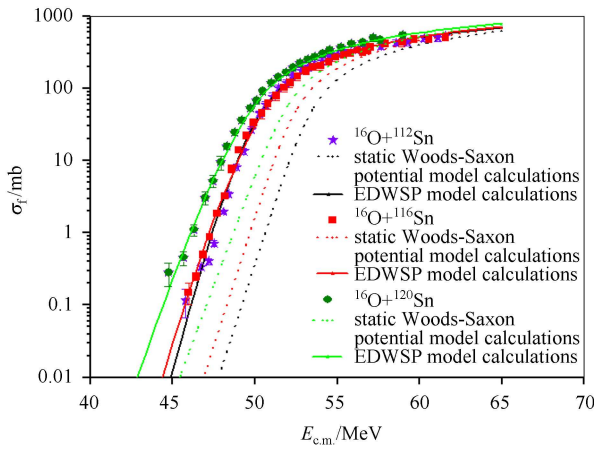

Fig. 4. (color online) The comparison of fusion excitation functions of $^{16}_{8}$O+$^{112,116,120}_{50}$Sn systems obtained using the static Woods–Saxon potential model and the energy-dependent Woods–Saxon potential model (EDWSP model) in conjunction with the one-dimensional Wong formula. The results are compared with available experimental data (symbols) taken from Ref. [42–44].

In coupled channel calculations, a larger value of diffuseness parameter $a \approx 0.83$ fm is required to reproduce the sub-barrier fusion enhancement. In a similar fashion, in EDWSP model calculations, significantly larger values of the diffuseness parameter ranging from a=0.85 fm to a=0.96 fm are needed for a complete description of the sub-barrier fusion data. This clearly indicates that the energy-dependence in the Woods–Saxon potential mirrors similar features of heavy ion fusion reactions as extracted from the static Woods–Saxon potential with large diffuseness parameter. Ghodsi et al. [54] have shown that the M3Y+repulsion and static Woods–Saxon potential with large diffuseness parameter accurately reproduce the sub-barrier fusion dynamics and hence the effects of M3Y+repulsion potential can be accurately reproduced by a static Woods–Saxon potential with abnormally large diffuseness parameter ranging from a=0.75 fm to a=1.5 fm. The similarity between the M3Y+repulsion potential and static Woods–Saxon potential with large diffuseness parameter are also reflected in the work of Esbensen et al. [55–58] and Stefanini et al. [59, 60]. In the eigen-channel approximation, the effect of coupling between relative motion of colliding nuclei and internal structure degrees of freedom is to replace the Coulomb barrier into a spectrum of barriers. The probability of penetration through barriers whose heights are lower than that of the fusion barrier is quite large. This spectrum of barriers is the fingerprint of fusion enhancement at below-barrier energies. In a similar way, the EDWSP model produces a distribution of barriers of varying heights (see Fig. 2) and hence reasonably addresses the fusion enhancement at sub-barrier energies.

4 Conclusions

The static Woods–Saxon potential and the energy-dependent Woods–Saxon potential are simultaneously used along with the one-dimensional Wong formula for addressing the fusion dynamics of $^{16}_{8}$O+$^{112,116,120}_{50}$Sn systems. The role of multi-phonon vibrational states is found to have a significant contribution in the enhancement of the sub-barrier fusion cross-section with respect to the expectation of the one-dimensional barrier penetration model. Although Sn-isotopes have a similar structure of low-lying surface vibrational states, the larger sub-barrier fusion enhancement of the $^{16}_{8}$O+$^{120}_{50}$Sn system in comparison to the $^{16}_{8}$O+$^{112,116}_{50}$Sn systems is a consequence of the strong collective nature of heavier target nuclei. The theoretical calculations based on the static Woods–Saxon potential within the context of the one-dimensional Wong formula systematically fail to reproduce the fusion dynamics of these systems. On the other hand, the energy-dependent Woods–Saxon potential model (EDWSP model) in conjunction with the one-dimensional Wong formula adequately addresses the sub-barrier fusion enhancement of $^{16}_{8}$O+$^{112,116,120}_{50}$Sn systems. In EDWSP model calculations, larger values of diffuseness parameter ranging from a=0.85 fm to a=0.96 fm are required to account for the fusion data. This unambiguously indicates that the energy-dependent Woods–Saxon potential is effectively equivalent to that of the static Woods–Saxon potential with abnormally large diffuseness.

References

1 Beckerman M. Rep. Prog. Phys., 1988, **51**: 1047
2 Reisdorf W. J. Phys. G, 1994, **20**: 1297
3 Dasgupta M et al. Annu. Rev. Nucl. Part. Sci., 1998, **48**: 401
4 Balantekin A B, Takigawa N. Rev. Mod. Phys., 1988, **70**: 77
5 Canto L F et al. Phys. Rep., 2006, **424**: 1
6 Hagino K, Takigawa N. Prog. Theor. Phys., 2012, **128**: 1061
7 Back B B et al. Rev. Mod. Phys., 2014, **86**: 317
8 Timmers H et al. Phys. Lett. B, 1997, **399**: 35
9 Trotta M et al. Phys. Rev. C, 2001, **65**: 011601
10 Stefanini A M et al. Phys. Rev. C, 2007, **76**: 014610
11 Leigh J R et al. Phys. Rev. C, 1995, **52**: 3151
12 Prasad N V S V et al. Nucl. Phys. A, 1996, **603**: 176
13 ZHANG H Q et al. Phys. Rev. C, 2010, **82**: 054609
14 Newton J O et al. Phys. Rev. C, 2001, **64**: 064608
15 Sonzogni A A et al. Phys. Rev. C, 1998, **57**: 722
16 Dasso C H, Pollarolo G. Phys. Rev. C, 2003, **68**: 054604
17 Hagino K et al. Phys. Rev. C, 2003, **67**: 054603
18 Sagaidak R N et al. Phys. Rev. C, 2007, **76**: 034605
19 WANG N, Scheid W. Phys. Rev. C, 2008, **78**: 014607
20 Ghodsi O N, Gharaei R. Eur. Phys. J. A, 2012, **48**: 21
21 Duhan S S, Singh M, Kharab R. Mod. Phys. Lett. A, 2011, **26**: 1017
22 Duhan S S, Singh M, Kharab R. Int. J. Mod. Phys. E, 2012, **21**: 1250054
23 Duhan S S, Singh M, Kharab R. Commun. Theor. Phys., 2011, **55**: 649
24 Duhan S S, Singh M, Kharab R. Phys. At. Nucl., 2011, **74**: 49
25 Newton J O et al. Phys. Rev. C, 2004, **70**: 024605
26 Hagino K, Rowley N. Phys. Rev. C, 2004, **69**: 054610
27 Mukherjee A et al. Phys. Rev. C, 2007, **75**: 044608
28 Chushnyakova M V, Bhattacharya R, Gontchar I I. Phys. Rev. C, 2014, **90**: 017603
29 Gontchar I I, Bhattacharya R, Chushnyakova M V. Phys. Rev. C, 2014, **89**: 034601
30 Singh M, Duhan S S, Kharab R. Mod. Phys. Lett. A, 2011, **26**: 2129
31 Sukhvinder M Singh, Kharab R. Nucl. Phys. A, 2013, **897**: 179
32 Sukhvinder M Singh, Kharab R. Nucl. Phys. A, 2013, **897**: 198
33 Sukhvinder M Singh, Kharab R. AIP Conf. Proc., 2013, **1524**: 163
34 Singh M, Sukhvinder, Kharab R, Atti Della "Fondazione Giorgio Ronchi" Anno LXV, 2010, **6**: 751
35 Singh M, Phil M. Dissertation (2009) (unpublished), Kurukshetra University Kurukshetra, Haryana, India
36 Singh M, Ph.D, Thesis, (2013) (unpublished), Kurukshetra University, Kurukshetra, Haryana, India, 2013
37 Singh M, Kharab R. EPJ Web of Conferences, 2014, **66**: 03043
38 Gautam M S. Phys. Rev. C, 2014, **90**: 024620
39 Gautam M S. Nucl. Phys. A, 2015, **933**: 272
40 Gautam M S. Phys. Scr., 2015, **90**: 025301, Phys. Scr., 2015, **90**: 055301
41 Gautam M S. Mod. Phys. Lett. A, 2015, **30**: 1550013; Acta Phys. Pol. B, 2015, **46**: 1055; Can. J. Phys., 2015, **93**: 1
42 Tripathi V et al. Phys. Rev. C, 2001, **65**: 014614
43 Baby L T et al. Phys. Rev. C, 2000, **62**: 014603
44 Sinha S et al. Phys. Rev. C, 2001, **64**: 024607
45 Wong C Y. Phys. Rev. Lett., 1973, **31**: 766
46 Hagino K, Rowley N, Kruppa A T. Comput. Phys. Commun., 1999, **123**: 143
47 Hill D L, Wheeler J A. Phys. Rev., 1953, **89**: 1102
48 Hagino K et al. Phys. Rev. C, 1997, **55**: 276
49 Hagino K et al. J. Phys. G, 1997, **23**: 1413
50 Esbensen H, Fricke S H, Landowne S. Phys. Rev. C, 1989, **40**: 2046
51 Hagino K et al. Phys. Rev. C, 1998, **57**: 1349
52 Zamrun F M et al. Phys. Rev. C, 2010, **81**: 044609
53 Anjos R M et al. Phys. Rev. C, 1990, **42**: 354
54 Ghodsi O N, Zanganeh V. Nucl. Phys. A, 2010, **846**: 40
55 Esbensen H, JIANG C L, Stefanini A M. Phys. Rev. C, 2010, **82**: 054621
56 Esbensen H, JIANG C L, Stefanini A M. Phys. Rev. C, 2014, **89**: 044606
57 Esbensen H, JIANG C L. Phys. Rev. C, 2009, **79**: 064619
58 Esbensen H, Misicu S. Phys. Rev. C, 2007, **76**: 054609
59 Stefanini A M et al. Phys. Lett. B, 2009, **679**: 95
60 Stefanini A M et al. Phys. Lett. B, 2014, **728**: 639